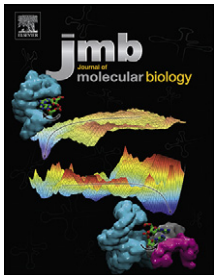

A Similar *In Vitro* and In Cell Lysate Folding Intermediate for the FF Domain

Michael P. Latham[1] **and Lewis E. Kay**[1,2]

*1 - **Departments of Molecular Genetics,** Biochemistry and Chemistry, University of Toronto, Toronto, ON M5S 1A8, Canada*
*2 - **Program in Molecular Structure and Function,** Hospital for Sick Children, Toronto, ON M5G 1X8, Canada*

***Correspondence to Lewis E. Kay:** Departments of Molecular Genetics, Biochemistry and Chemistry, University of Toronto, Medical Sciences Building, Room 1233, 1 King's College Circle, Toronto, ON M5S 1A8, Canada. kay@pound.med.utoronto.ca*
http://dx.doi.org/10.1016/j.jmb.2014.07.019
Edited by C. Kalodimos

Abstract

Understanding the mechanisms by which proteins fold into their three-dimensional structures, including a description of the intermediates that are formed during the folding process, remains a goal of protein science. Most studies are performed under carefully controlled conditions in which the folding reaction is monitored in a buffer solution that is far from the natural milieu of the cell. Here, we have used ^{13}C and ^{1}H relaxation dispersion NMR spectroscopy to study folding of the FF domain in both *Escherichia coli* and *Saccharomyces cerevisiae* cellular lysates. We find that a conformationally excited state is populated in both lysates, which is very similar in structure to a folding intermediate observed in previous studies in buffer, with the kinetics and thermodynamics of the interconversion between native and intermediate conformers somewhat changed. The results point to the importance of extending folding studies beyond the test tube yet emphasize that insights can be obtained through careful experiments recorded in controlled buffer solutions.

The majority of cellular proteins fold into an ensemble of conformers that are important for function. Folding is governed by an energy landscape that dictates the process by which a newly translated nascent chain evolves to its final functional structure [1–3]. Along the way, the protein may visit higher energy and transiently formed intermediate states whose characterization is important for a detailed understanding of the folding mechanism [3]. Once folded, excursions from the native state to sparsely populated, transiently formed conformers can also occur, and these have been shown to be important for a variety of biological processes, including ligand binding, catalysis, molecular recognition and allostery [4–7]. The natural setting for these processes is not the homogeneous environment of the test tube, where the vast majority of structural and biophysical measurements have been carried out, but rather the crowded and heterogeneous cellular milieu, where active (chaperones and unfoldases) and passive (crowding and non-specific interactions) forces act to perturb the energy landscape [8,9]. The effect of these forces can alter protein thermodynamics, kinetics and structure relative to what is measured *in vitro*. It therefore becomes critical to study dynamical processes, such as protein folding, in an environment more relevant than buffer.

NMR spectroscopy is well suited to study protein structure and dynamics *in vivo* or in "cell-like" environments, and a number of compelling examples have been reported [10–16]. Here, we are interested in extending such studies to folding pathways and the characterization of "invisible" protein conformers that are visited from the native state and play important roles in both folding and misfolding processes. In particular, we present a folding study of the four-helix-bundle FF domain from human HYPA/FBP11 [17] in cell lysate using Carr–Purcell–Meiboom–Gill (CPMG) [18,19] relaxation dispersion (RD) [20] NMR spectroscopy and compare results with those obtained in similar analyses performed in buffer.

Previously we have used a suite of CPMG RD NMR experiments to study the folding of the FF domain dissolved in buffer [21,22], a process that proceeds via formation of an on-pathway intermediate (*I*) [23] (Fig. 1). The intermediate state cannot be

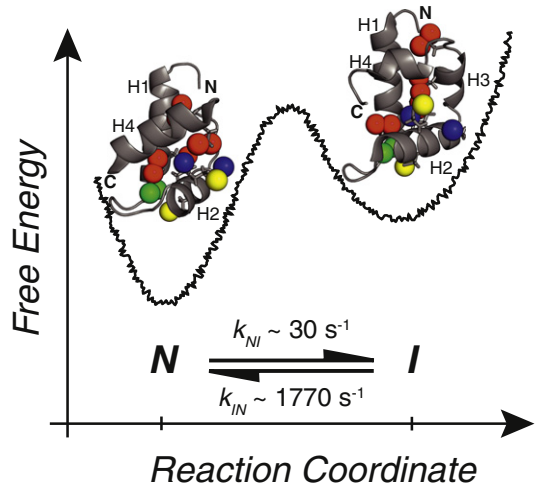

Fig. 1. Schematic representation of the simplified conformational energy landscape for the FF domain *N*-to-*I* transition. Three-dimensional structures of the *N* (PDB ID 1UZC [23]) and *I* (PDB ID 2KZG [21]) states are shown above their respective free-energy minima. Ile(δ1), Leu(δ), Val(γ) and Met(ε) methyl groups are shown using blue, red, green and yellow spheres, respectively. Conformational exchange rate constants, obtained from CPMG RD data at 30 °C, are given below the minima. RD data were analyzed using an in-house written program (ChemEx, available upon request) following an approach detailed in the literature [40,41] and described in Supporting Information.

observed directly in NMR spectra due to its low population (~2% at 30 °C) and short lifetime (~0.5 ms). However, because *I* exchanges with the native, highly populated ground state (*N*), $I \underset{k_{NI}}{\overset{k_{IN}}{\rightleftharpoons}} N$, at a rate $k_{ex} = k_{NI} + k_{IN} = \sim 1800\ s^{-1}$, it can be studied indirectly through broadening of the correlations in spectra of the ground-state conformation. The broadening, in turn, is manipulated as a function of the frequency of application of chemical shift refocusing pulses, ν_{CPMG}, producing dispersion profiles [20], $R_{2,eff}$ *versus* ν_{CPMG}, that have been analyzed previously to obtain the kinetics and thermodynamics of the interconversion and near-complete backbone ^{1}H, ^{15}N and ^{13}C chemical shifts of *I*. These have been used to generate three-dimensional models of the intermediate-state structure [21]. Notably, significant differences between *I* and *N* are observed in helices H3 and H4 that lead to a series of non-native interactions (Fig. 1). These involve residues A17, A20 and L24 of H1 and residues L52 and L55 in H3 that form different contacts in *I* and *N*, with an additional non-native hydrophobic cluster involving residues A53, Y49 and I44 [21,22].

In order to establish whether FF domain folding proceeds via a similar non-native intermediate in a cell-like environment, we have used sensitive methyl side-chain ^{13}C and ^{1}H CPMG RD experiments [24,25] recorded on samples dissolved in lysate, as opposed to *in vivo* measurements. This allows us to use sufficiently high FF concentrations (1–2 mM) to obtain adequate spectral signal to noise for a detailed, quantitative analysis and obviates the worry of leakage from dead or damaged cells [26] that would otherwise accompany the lengthy experiments (1–3 days). Cell lysates are not a true *in vivo* environment and do not include separate compartments nor the cytoskeletal matrix that most certainly can play important roles in protein function [27]. Moreover, the protein concentrations that must be used to obtain the requisite sensitivity for the CPMG experiments described herein are much higher than would typically be found *in vivo*. The lysate environment that has been chosen for the studies described presently is best thought of as a bridge between *in vitro* and *in vivo*, in which quantitative experiments that are sensitivity limited can be performed to obtain insight into the effects of both small metabolites and biomolecules on processes such as protein folding.

Figure 2 shows an overlay of two-dimensional (2D) ^{13}C–^{1}H spectra of FF in buffer (blue single contour) or *Escherichia coli* lysate (red contours), with an excellent correlation between the positions of peaks in each spectrum. We have noted in samples of *E. coli* lysate preparations that extra peaks arising from FF domain degradation products emerge rapidly, denoted by asterisks in Fig. 2. These likely reflect the increased labiality that arises from the interconversion to an intermediate state that is less well protected from proteolysis than *N*, although we cannot, of course, be certain that degradation does not also proceed from the native conformation. Degradation to this extent was not observed in our previous studies involving the protein calmodulin in lysate [13,28], emphasizing that studies of "delicate" systems such as those involving folding intermediates must proceed as rapidly as possible (see below and Supporting Information).

Figure 3 shows representative methyl ^{13}C (a) and ^{1}H (b) RD profiles recorded on U-^{2}H,^{15}N; Ile(δ1), Leu(δ), Val(γ) and Met(ε) –$^{13}CH_3$ (^{13}C RD) or –$^{13}CHD_2$ (^{1}H RD) labeled samples of the FF domain, respectively, dissolved in either phosphate buffer (pH 6.8, closed circles) or 100 g/L *E. coli* lysate (pH 6.5, open circles), 30 °C. For both methyl ^{13}C and ^{1}H probes, $R_{2,eff}$ at the highest ν_{CPMG} value is greater in lysate than in buffer, reflecting the increased macromolecular tumbling time for the FF domain in the viscous lysate solution. Also of interest, RD profiles are observed in lysate samples of the FF domain for L24, L52, L55 and I44, which have been observed to participate in non-native interactions in the *I* state in studies of FF dissolved in buffer [21,22]. ^{13}C and ^{1}H RD profiles recorded at a pair of static magnetic fields (14.1 and 18.8 T) were fit to a two-state model of conformational exchange to extract the

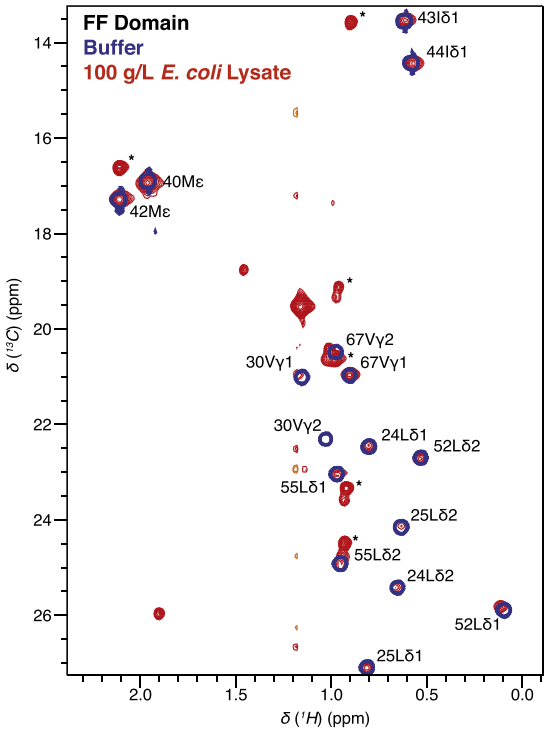

Fig. 2. The "average" structure of the *N* state is unaffected in *E. coli* lysate. Overlay of 2D ^{13}C–^{1}H correlation spectra of U-[^{2}H,^{15}N]; Ile(δ1)-[$^{13}CH_3$], Leu(δ)/Val(γ)-[$^{13}CH_3$,$^{12}CD_3$], Met(ε)-[$^{13}CH_3$] labeled FF domain, prepared as previously described [22], recorded at 14.1 T, 30 °C on samples dissolved in buffer (25 mM sodium phosphate, pH 6.8, 50 mM NaCl, 1 mM ethylenediaminetetraacetic acid, 100% D_2O; single blue contours) or 100 g/L *E. coli* lysate (red contours). *E. coli* lysate was prepared as previously described [13] with the small-molecule (<3 kDa) fraction added back to the concentrated lysate stock solution. Concentrated stock solutions of FF and lysate were subsequently mixed yielding 1–1.5 mM FF domain in solution with 100 g/L *E. coli* lysate proteins. Methyl side-chain assignments are given [23]. Peaks labeled with an asterisk arise from FF domain degradation in the lysate. Further details can be found in Supporting Information.

population of *I* (p_I), the exchange rate (k_{ex}) and the absolute values of chemical shift differences between nuclei in the *N* and *I* states. Similar exchange parameters were obtained from fits of the ^{13}C and ^{1}H profiles in buffer, k_{ex} = 1880 ± 40 s^{-1}/p_I = 1.5 ± 0.4% (reduced χ^2 = 1.05) and k_{ex} = 1720 ± 20 s^{-1}/p_I = 1.8 ± 0.2% (reduced χ^2 = 0.91), respectively. The corresponding parameters in *E. coli* lysate are k_{ex} = 1050 ± 40 s^{-1}/p_I = 2.3 ± 0.7% (^{13}C RD; reduced χ^2 = 1.01) and k_{ex} = 1270 ± 20 s^{-1}/p_I = 2.8 ± 0.2% (^{1}H RD; reduced χ^2 = 0.90); note that separate lysate samples were prepared for the ^{13}C ($^{13}CH_3$) and ^{1}H ($^{13}CHD_2$) RD experiments. In order to estimate the errors in fitted exchange parameters, we have carried out a bootstrap analysis (Fig. S1) as described in Supporting Information. Notably, there is little correlation between p_I and k_{ex} implying that the differences in k_{ex} values observed in buffer (~1800 s^{-1}) and lysate (~1150 s^{-1}) are not a fitting artifact. As described above (and in Supporting Information in more detail), the CPMG analysis is based on a two-site exchange mechanism that has previously been shown to be valid in studies of wild-type FF domain folding in buffer [21,29]. The reduced χ^2 values suggest that such a model is adequate for the analyses of dispersion profiles recorded in *E. coli* lysate as well. Finally, we have established that the extracted exchange parameters are robust to the effects of sample degradation over the time course used in our studies by recording spectra at static magnetic field strengths of 14.1 and 18.8 T consecutively, with the same exchange values and chemical shift differences obtained in both cases.

The smaller exchange rate constant for the interconversion between *N* and *I* that has been measured in lysate is not unexpected due to the increased viscosity relative to buffer. Previous work [29] has shown that the exchange between *N* and *I* can be well described by a modified version of Kramers' equation [30,31]

$$k_{ij} = A_{ij}/(\eta + \sigma)$$

where *A* is a constant that contains, among other terms, an exponent of the activation free energy for the reaction, and η and σ are the contributions to the viscosity along the reaction coordinate from solvent and intra-protein (internal) interactions, respectively. For FF domain folding, σ is considerably smaller than the viscosity of water, consistent with an $N \rightleftharpoons I$ interconversion that is driven predominantly by water dynamics [29]. Further studies establish that FF domain folding involves a small-length-scale diffusive process, with an effective hydrodynamic radius on the order of an amino acid side chain [29,32]. Thus, the viscosity along the reaction coordinate that describes the FF domain interconversion would be predicted to be that "felt" by a small-molecule probe (<5 Å) dissolved in the lysate, assuming that the lysate is an inert viscogen. Translational diffusion coefficients for a number of small-molecule probes ranging in size from 1.5 to 3.0 Å were measured in 100 g/L *E. coli* lysate (see Supporting Information) and a uniform increase in viscosity on the order of 40% was obtained relative to values in buffer. Assuming that k_{ex} for the FF domain scales inversely with viscosity along the reaction coordinate, as has been shown previously [29], a decrease in rate to ~1300 s^{-1} that is only slightly higher than what is observed in lysate is calculated.

A significant difference in p_I between lysate and buffer has been obtained, 2.6% and 1.7%, respectively, indicating that the stability of *I* relative to *N* increases in lysate (Fig. S1). This difference in stability does not derive from a change in compaction. For

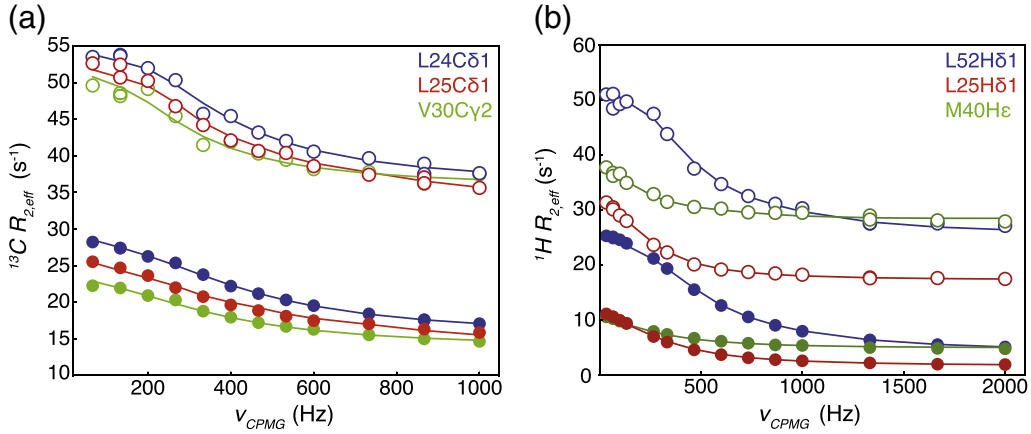

Fig. 3. Monitoring the *I*-to-*N* transition in a biological environment. Representative ^{13}C (a) and ^{1}H (b) CPMG RD profiles [24,25] for the FF domain dissolved in buffer (filled circles) or 100 g/L *E. coli* lysate (open circles). These data were recorded at 14.1 T, 30 °C with a constant time relaxation delay of 30 ms using U-^{2}H,^{15}N; Ile(δ1), Leu(δ), Val(γ) and Met(ε) –$^{13}CH_3$ (a) or –$^{13}CHD_2$ (b) labeled samples of FF domain. Additional CPMG RD data sets were also collected at 18.8 T utilizing a 30-ms constant time relaxation delay. We recorded 15 (17) CPMG frequencies between 33.3 and 1000 Hz (2000 Hz) for ^{13}C (^{1}H) RD data sets with two repeat frequencies for error analysis. Data sets were processed with NMRPipe, and peak intensities were subsequently quantified with the nlinLS utility [42]. Continuous lines represent fits to a two-state exchange model generated with ChemEx. Further details regarding the data fitting are provided in the legend of Fig. 4 and Supporting Information.

example, considering only the folded core of the four-helix bundle (residues 11–66), *N* is more compact than *I* (volumes of ~6900 *versus* ~7600 Å^3, respectively). An even larger difference in compactness is expected when the complete sequence is taken into account as the C-terminus of the *I* state is partially disordered [21]. It would therefore be predicted from excluded volume effects that *I* would be further destabilized relative to *N* in lysate, in contrast to what is observed experimentally. Rather, the differences in relative stabilities of exchanging states in lysate and buffer most likely reflect non-specific interactions between FF and the large variety of molecular components of the lysate. Of note in this regard is that the FF domain has a theoretical pI of 9.8 and hence would be positively charged at the pH used here (6.5), while the majority of proteins in *E. coli* lysate have pI values below 7 so that at least some of them are expected to be negatively charged [33] and hence likely to form electrostatic-based contacts with the FF domain. In this regard, it is of interest to note that calculations suggest that *I* exposes a larger solvent-accessible surface area for charged side chains (~920 Å^2) compared to *N* (~740 Å^2). Of course, these non-specific interactions could be mediated through hydrophobic contacts as well. Regardless of the mechanism, such interactions do not manifest in changes in ^{13}C–^{1}H correlation spectra of FF in lysate (Fig. 2) because they are sufficiently transient and weak so as not to change the average structure as reported by methyl group chemical shifts and/or because interactions involve regions that lack I,L,V, M methyl group reporters. Interestingly, the interactions do, in some cases, affect relative intensities of correlations that decrease in the lysate environment (e.g., L24, L25, V30). As has recently been discussed, predicting non-specific interactions in the context of a complex biological environment based on net charges of the molecular players can be difficult [34]. Further, it was suggested that proteins may possess natural affinities for each other in general, with interaction constants that are distinct from what is routinely measured under homogeneous, dilute buffer conditions [34].

In addition to k_{ex} and p_I, methyl ^{13}C and ^{1}H chemical shift differences between *N* and *I* ($|\Delta\nu_{CPMG}| = |\nu_I - \nu_N|$; in Hz, 14.1 T) have been extracted from fits of RD data. Figure 4a shows the correlation between $|\Delta\nu_{CPMG}|$ values that has been obtained from fits of RD profiles recorded in buffer and lysate. Chemical shifts are exquisitely sensitive to molecular structure so that the excellent correlation between $|\Delta\nu_{CPMG}|$ values (root-mean-square deviation, r.m.s.d., <20 Hz) provides strong evidence that the conformationally excited states populated in both buffer and lysate are very similar. By means of comparison, a relatively poor correlation (r.m.s.d. = 81 Hz) is obtained when shift differences from FF in lysate are compared with predicted $|\Delta\nu|$ values that have been calculated under the assumption that the minor state is unfolded (Fig. 4a, inset) [35]. Thus, the sparsely populated conformer characterized in *E. coli* lysate corresponds closely to the on-pathway folding intermediate that has been studied previously in buffer. Although the thermodynamics and, to a much smaller extent, also the kinetics of the FF domain

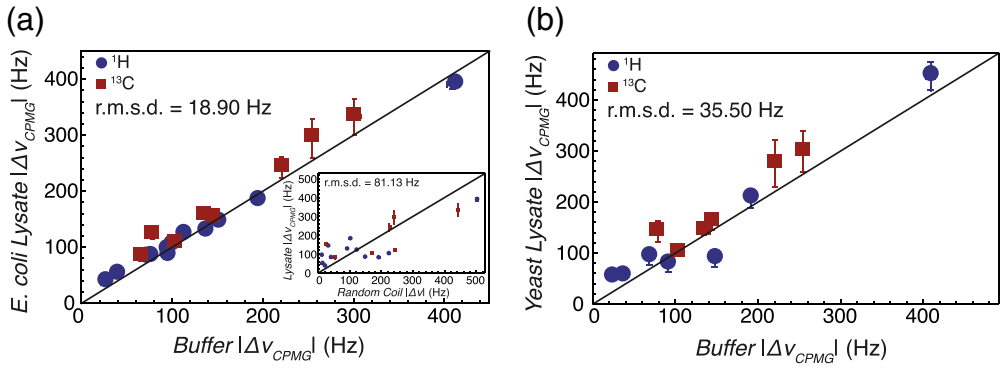

Fig. 4. Similar folding intermediates for the FF domain in buffer and in "cell-like" environments. Comparison of $|\Delta\nu_{CPMG}|$ values from fits of RD profiles recorded on FF domain samples dissolved in *E. coli* (a) or *S. cerevisiae* (b) lysate relative to shift differences from samples dissolved in buffer. Blue circles and red squares represent $|\Delta\nu_{CPMG}|$ values of ^{1}H and ^{13}C nuclei, respectively. Chemical shift data were obtained from fits of the CPMG RD data to a two-state exchange model as described previously [40,41], by numerically simulating the Bloch-McConnell equations [43] through the constant time relaxation delay. Global (k_{ex}, exchange rate constant $k_{NI} + k_{IN}$; p_I, fractional population of *I*) and local [$|\Delta\varpi|$, chemical shift difference between resonances interconverting between *I* and *N* in parts per million (ppm); $R_{2,\infty}$, transverse relaxation rate at infinite ν_{CPMG}; I_0, initial magnetization intensity] exchange parameters were obtained by minimizing a χ^2 target fitting function. While CPMG RD data sets collected at two static magnetic fields (14.1 and 18.8 T) were fitted together, RD data for each nucleus (^{13}C or ^{1}H) at each solution condition (buffer or lysate) were analyzed individually. The inset to (a) shows $|\Delta\nu_{CPMG}|$ from the FF domain in lysate plotted against predicted values, assuming that the excited-state chemical shifts are given by random-coil values for ^{13}C (red squares) and ^{1}H (blue circles) [35].

transition are altered between the buffer and lysate environments, both the *N* and *I* states appear to be essentially unchanged. This provides strong evidence that the interconversion studied in *E. coli* lysate corresponds to the folding reaction that has been characterized in buffer previously. Additionally, the strong correlation between buffer and lysate chemical shifts observed for both *I* (Fig. 4a) and *N* (Fig. 2) suggests that both states have only very weak and transient interactions with the molecular components of the *E. coli* lysate. In this limit (fast exchange with lysate), the *N,I* interconversion would still be described by a simple two-state exchange model, as observed here.

It is of interest to establish whether the FF domain folding intermediate observed in buffer and *E. coli* lysate is also present in other lysate environments. This is particularly germane because the FF domain is a phosphoserine/phosphothreonine binding module that is found in eukaryotic mRNA splicing factors [36] so that *E. coli* lysate is not the natural milieu for its function. We have therefore repeated the methyl RD NMR experiments using FF dissolved in 100 g/L lysate from *Saccharomyces cerevisiae* that is a more representative environment. As with *E. coli* lysate, 2D ^{13}C–^{1}H correlation spectra of the FF domain dissolved in *S. cerevisiae* lysate are very similar to their counterparts in buffer (Fig. S2). Unlike the *E. coli* lysate, the *S. cerevisiae* lysate generates considerable background signals in 2D ^{13}C–^{1}H correlation spectra that limited the number of ^{13}C and ^{1}H RD profiles that could be quantified to 8 and 9, respectively, down by approximately 60% from the number in *E. coli* lysate. Recorded ^{13}C and ^{1}H CPMG RD profiles (Fig. S3) were analyzed using the two-state exchange model described above, yielding exchange parameters of $k_{ex} = 860 \pm 80\ s^{-1}/p_I = 2.8 \pm 0.2\%$ (^{13}C RD; reduced $\chi^2 = 1.05$) and $k_{ex} = 720 \pm 100\ s^{-1}/p_I = 2.6 \pm 0.2\%$ (^{1}H RD; reduced $\chi^2 = 1.05$) (Fig. S1). Similar to our study using *E. coli* lysate, the intermediate population is increased relative to buffer, consistent with a relative stabilization of *I* with respect to *N*. Notably, the exchange rate is significantly decreased from that measured for the *I*-to-*N* folding reaction in buffer (~1800 s^{-1}) and cannot be explained by the ~25% increase in viscosity that is measured for probe molecules dissolved in a sample of 100 g/L *S. cerevisiae* lysate. It is therefore clear that the barrier for FF *I*-to-*N* interconversion is increased in this lysate environment. Such an increase likely reflects interactions between the FF domain and lysate proteins. Notably, non-specific contacts between Ca^{2+}-bound calmodulin (Ca-CaM) and endogenous proteins of *S. cerevisiae* lysate have been observed previously [28].

Despite the change in the exchange parameters, a good correlation between $|\Delta\nu_{CPMG}|$ values from fits of ^{13}C and ^{1}H RD data recorded on the FF domain dissolved in *S. cerevisiae* lysate and in buffer is obtained (Fig. 4b) (r.m.s.d. = 36 Hz). Thus, very similar FF domain folding intermediates are present in buffer, *E. coli* and *S. cerevisiae* lysates, consistent with similar folding mechanisms in the three distinct environments.

Several protein folding studies have been performed *in vivo* or under conditions that are "in cell-like" using a variety of techniques such as fluorescence

microscopy and NMR spectroscopy [12,16,37–39]. These studies generally focused on global unfolding processes and provide examples of both native-state stabilization and destabilization. For instance, Gruebele *et al*. have shown that folded phosphoglycerate kinase is more stable *in vivo* and attribute the increased stability to differences in local viscosity and/or hydrophobicity of the cellular environment [38,39]. Interestingly, Pielak *et al*. have observed that the negatively charged chymotrypsin inhibitor 2 protein is destabilized in a solution comprised of only negatively charged proteins from *E. coli* lysate despite the fact that charge repulsions are predicted to stabilize proteins [12,34]. Also of note, Shirakawa *et al*. have found that both specific and non-specific interactions play a role in destabilizing ubiquitin in HeLa cells [16]. Here, we have shown that, for the FF domain, the relative stability of *I versus N* increases slightly in cellular lysate relative to buffer. The high theoretical pI value for the FF domain (9.8) suggests that changes in electrostatic interactions, mediated through differences in side-chain packing between the two states, play a role in modulating the relative stability of the two states. It is clear that the impact of the cellular environment on protein folding, and on the intermediates that become transiently populated along the pathway, must be considered on a case-by-case basis.

In summary, we have shown that the FF domain dissolved in buffer, *E. coli* and *S. cerevisiae* lysates, populates similar conformationally excited states. Detailed studies in buffer establish that this state is an on-pathway folding intermediate [21,22] suggesting similar FF domain folding pathways in buffer and lysate. The kinetics and thermodynamics of the *I*-to-*N* interconversion, however, are somewhat perturbed. This work emphasizes the importance of studies in "cell-like" environments while illustrating that, at least in the case of the FF domain, similar folding intermediates exist *in vitro* and in lysate. Moreover, it also highlights the utility of NMR RD methodologies to probe folding process in complex heterogeneous solutions and to obtain detailed site-specific information about the intermediate states that are formed.

Supporting information

A description of protein expression, purification, lysate production, NMR experiments and data analysis is provided, as well as figures of spectra, RD profiles and goodness of RD fits.

Acknowledgments

M.P.L. acknowledges support in the form of post-doctoral fellowships from the National Science Foundation (OISE-0853108) and the Canadian Institutes of Health Research Training Grant in Protein Folding and Disease. Dr. John Rubinstein (Hospital for Sick Children) is thanked for providing laboratory space. This work was funded through Canadian Institutes of Health Research and Natural Sciences and Engineering Research Council of Canada research grants to L.E.K. L.E.K. holds a Canada Research Chair in Biochemistry.

Appendix A. Supplementary data

Supplementary data to this article can be found online at http://dx.doi.org/10.1016/j.jmb.2014.07.019.

Received 13 June 2014;
Received in revised form 21 July 2014;
Accepted 22 July 2014
Available online 30 July 2014

Keywords:
protein folding;
CPMG relaxation dispersion;
methyl side-chain;
in cell-like NMR

Abbreviations used:
CPMG, Carr–Purcell–Meiboom–Gill; RD, relaxation dispersion; 2D, two-dimensional.

References

[1] Frauenfelder H, Sligar SG, Wolynes PG. The energy landscapes and motions of proteins. Science 1991;254:1598–603.
[2] Dill KA. Dominant forces in protein folding. Biochemistry 1990;29:7133–55.
[3] Dill KA, Chan HS. From Levinthal to pathways to funnels. Nat Struct Biol 1997;4:10–9.
[4] Fraser JS, Clarkson MW, Degnan SC, Erion R, Kern D, Alber T. Hidden alternative structures of proline isomerase essential for catalysis. Nature 2009;462:669–73.
[5] Boehr DD, Dyson HJ, Wright PE. An NMR perspective on enzyme dynamics. Chem Rev 2006;106:3055–79.
[6] Karplus M, Kuriyan J. Molecular dynamics and protein function. Proc Natl Acad Sci USA 2005;102:6679–85.
[7] Eisenmesser EZ, Millet O, Labeikovsky W, Korzhnev DM, Wolf-Watz M, Bosco DA, et al. Intrinsic dynamics of an enzyme underlies catalysis. Nature 2005;438:117–21.
[8] Gershenson A, Gierasch LM. Protein folding in the cell: challenges and progress. Curr Opin Struct Biol 2011;21:32–41.
[9] Zhou H-X. Protein folding in confined and crowded environments. Arch Biochem Biophys 2008;469:76–82.
[10] Sakakibara D, Sasaki A, Ikeya T, Hamatsu J, Hanashima T, Mishima M, et al. Protein structure determination in living cells by in-cell NMR spectroscopy. Nature 2009;458:102–5.
[11] Reckel S, Hansel R, Lohr F, Dötsch V. In-cell NMR spectroscopy. Prog Nucl Magn Reson Spectrosc 2007;51:91–101.
[12] Sarkar M, Smith AE, Pielak GJ. Impact of reconstituted cytosol on protein stability. Proc Natl Acad Sci USA 2013;110:19342–7.

[13] Latham MP, Kay LE. Is buffer a good proxy for a crowded cell-like environment? A comparative NMR study of calmodulin side-chain dynamics in buffer and *E. coli* lysate. PLoS One 2012;7:e48226.
[14] Selenko P, Serber Z, Gadea B, Ruderman J, Wagner G. Quantitative NMR analysis of the protein G B1 domain in *Xenopus laevis* egg extracts and intact oocytes. Proc Natl Acad Sci USA 2006;103:11904–9.
[15] Danielsson J, Inomata K, Murayama S, Tochio H, Lang L, Shirakawa M, et al. Pruning the ALS-associated protein SOD1 for in-cell NMR. J Am Chem Soc 2013;135:10266–9.
[16] Inomata K, Ohno A, Tochio H, Isogai S, Tenno T, Nakase I, et al. High-resolution multi-dimensional NMR spectroscopy of proteins in human cells. Nature 2009;458:106–9.
[17] Allen M, Friedler A, Schon O, Bycroft M. The structure of an FF domain from human HYPA/FBP11. J Mol Biol 2002;323:411–6.
[18] Carr H, Purcell E. Effects of diffusion on free precession in nuclear magnetic resonance experiments. Phys Rev 1954; 94:630–8.
[19] Meiboom S, Gill D. Modified spin-echo method for measuring nuclear relaxation times. Rev Sci Instrum 1958;29:688.
[20] Palmer AG, Kroenke CD, Loria JP. Nuclear magnetic resonance methods for quantifying microsecond-to-millisecond motions in biological macromolecules. Methods Enzymol 2001; 339:204–38.
[21] Korzhnev DM, Religa TL, Banachewicz W, Fersht AR, Kay LE. A transient and low-populated protein-folding intermediate at atomic resolution. Science 2010;329:1312–6.
[22] Korzhnev DM, Religa TL, Lundström P, Fersht AR, Kay LE. The folding pathway of an FF domain: characterization of an on-pathway intermediate state under folding conditions by (15)N, (13)C(alpha) and (13)C-methyl relaxation dispersion and (1)H/(2)H-exchange NMR spectroscopy. J Mol Biol 2007;372:497–512.
[23] Jemth P, Day R, Gianni S, Khan F, Allen M, Daggett V, et al. The structure of the major transition state for folding of an FF domain from experiment and simulation. J Mol Biol 2005; 350:363–78.
[24] Lundström P, Vallurupalli P, Religa TL, Dahlquist FW, Kay LE. A single-quantum methyl 13C-relaxation dispersion experiment with improved sensitivity. J Biomol NMR 2007;38:79–88.
[25] Baldwin AJ, Religa TL, Hansen DF, Bouvignies G, Kay LE. (13)CHD(2) methyl group probes of millisecond time scale exchange in proteins by (1)H relaxation dispersion: an application to proteasome gating residue dynamics. J Am Chem Soc 2010;132:10992–5.
[26] Barnes CO, Pielak GJ. In-cell protein NMR and protein leakage. Proteins 2011;79:347–51.
[27] Ellis RJ. Macromolecular crowding: obvious but underappreciated. Trends Biochem Sci 2001;26:597–604.
[28] Latham MP, Kay LE. Probing non-specific interactions of Ca^{2+}-calmodulin in *E. coli* lysate. J Biomol NMR 2013; 55:239–47.
[29] Sekhar A, Vallurupalli P, Kay LE. Folding of the four-helix bundle FF domain from a compact on-pathway intermediate state is governed predominantly by water motion. Proc Natl Acad Sci USA 2012;109:19268–73.
[30] Hänggi P, Borkovec M. Reaction-rate theory: fifty years after Kramers. Rev Mod Phys 1990;62:251–341.
[31] Ansari A, Jones CM, Henry ER, Hofrichter J, Eaton WA. The role of solvent viscosity in the dynamics of protein conformational changes. Science 1992;256:1796–8.
[32] Sekhar A, Vallurupalli P, Kay LE. Defining a length scale for millisecond-timescale protein conformational exchange. Proc Natl Acad Sci USA 2013;110:11391–6.
[33] Schwartz R, Ting CS, King J. Whole proteome p*I* values correlate with subcellular localizations of proteins for organisms within the three domains of life. Genome Res 2001;11:703–9.
[34] Sarkar M, Lu J, Pielak GJ. Protein crowder charge and protein stability. Biochemistry 2014;53:1601–6.
[35] Wishart DS, Bigam CG, Holm A, Hodges RS, Sykes BD. 1H, 13C and 15N random coil NMR chemical shifts of the common amino acids. I. Investigations of nearest-neighbor effects. J Biomol NMR 1995;5:67–81.
[36] Carty SM, Goldstrohm AC, Suñé C, Garcia-Blanco MA, Greenleaf AL. Protein-interaction modules that organize nuclear function: FF domains of CA150 bind the phosphoCTD of RNA polymerase II. Proc Natl Acad Sci USA 2000; 97:9015–20.
[37] Hong J, Gierasch LM. Macromolecular crowding remodels the energy landscape of a protein by favoring a more compact unfolded state. J Am Chem Soc 2010;132:10445–52.
[38] Guo M, Xu Y, Gruebele M. Temperature dependence of protein folding kinetics in living cells. Proc Natl Acad Sci USA 2012;109:17863–7.
[39] Dhar A, Ebbinghaus S, Shen Z, Mishra T, Gruebele M. The diffusion coefficient for PGK folding in eukaryotic cells. Biophys J 2010;99:L69–71.
[40] Korzhnev DM, Salvatella X, Vendruscolo M, Di Nardo AA, Davidson AR, Dobson CM, et al. Low-populated folding intermediates of Fyn SH3 characterized by relaxation dispersion NMR. Nature 2004;430:586–90.
[41] Vallurupalli P, Hansen DF, Stollar E, Meirovitch E, Kay LE. Measurement of bond vector orientations in invisible excited states of proteins. Proc Natl Acad Sci USA 2007;104:18473–7.
[42] Delaglio F, Grzesiek S, Vuister GW, Zhu G, Pfeifer J, Bax A. NMRPipe: a multidimensional spectral processing system based on UNIX pipes. J Biomol NMR 1995;6:277–93.
[43] McConnell H. Reaction rates by nuclear magnetic resonance. J Chem Phys 1958;28:430.